Investigation on bioactivity, biocompatibility, thermal behavior and antibacterial properties of calcium silicate glass coatings containing Ag.

M. Catauro[1,*], F. Bollino[1], F. Papale[1], S. Vecchio Ciprioti[2]

[1]Department of Industrial and Information Engineering, Second University of Naples, Via Roma 29, 81031 Aversa, Italy

[2]Department of Basic and Applied Science for Engineering, Sapienza University of Rome, Via del Castro Laurenziano 7, Building RM017, I-00161 Rome, Italy

*Corresponding author: Michelina Catauro

Tel.: +39 081 5010360;

fax: +39 081 5010204.

E-mail address: michelina.catauro@unina2.it

Abstract

The aim of this study has been the preparation of dental implants with potential antibacterial properties. Bioactive glasses containing different percentages of silver have been synthesized via the sol-gel method and used to coat titanium implants by means of a dip coating technique. The glasses obtained have the following general formula, 70S30CxA, which is related to its composition (in mol%): 70% of SiO_2 (S), 30% of CaO (C) and x% of Ag_2O (A), with $0.08 \leq x \leq 0.27$. Fourier Transform InfraRed (FTIR) spectroscopy and simultaneous thermogravimetry/differential thermal analysis (TG/DTA) were used to characterize the materials. Scanning electron microscopy (SEM) has been used to investigate the coating morphology. Moreover, the films obtained have been characterized in order to verify their antibacterial activities as well as their bioactivity and biocompatibility as a function of Ag content. SEM/EDX analysis has shown that the films are bioactive because they are able to stimulate the hydroxyapatite nucleation on their surface when soaked in a simulated body fluid (SBF). WST-8 assay on 3T3 cells seeded on coated titanium substrates has proved that the coatings don't induce cytotoxicity. However, the results have shown that both the bioactivity and biocompatibility of coatings decrease slightly at high Ag contents. In contrast, antibacterial activity of the films against the *Staphylococcus aureus* increases with an increase of the silver amount.

Keywords: Silver-containing gel glass, bioactivity, antibacterial property, SEM, FTIR, TG/DTA.

1. Introduction

The septic loosening of a prosthesis is a serious failure that requires long-term antibiotic therapy, removal of the prosthesis and bone reconstructions. Bacterial contamination of dental or orthopedic implants is a serious complication that requires a heavy systemic antibiotic therapy, a second surgery to remove the infected prosthesis with a morbidity increase. The most common organism that causes infections in orthopedic implants is *Staphylococcus Aureus* (*S. Aureus*) [1]. Bacteria adhere on the implants surfaces and produce a biofilm, a complex structure made from bacteria and extracellular matrix that is capable of resisting antibiotics and host defences [2]. A massive antibiotic therapy or surgery is usually used to treat the infection; most implants infected with *S. aureus* require surgical removal [3] but this practice leads to musculoskeletal problems for the patient in the long term [4]. Replanting in two phases is the current standard of care for infected prostheses. It is associated with prolonged antibiotic therapy and two important operations. This causes an increase in patient morbidity and is an expensive protocol. The infected prosthesis is removed and spacers loaded with antibiotics are inserted. After 6 weeks the implantation of a new prosthesis is possible. The ideal solution would be to coat the prosthesis with a material capable of releasing antimicrobial agents *in situ* so as to avoid the onset of an infection focus. A well-known antimicrobial agent is silver. It exerts a strong antibacterial activity against many microbial strains without being toxic to human cells [5]. Silver has a broad spectrum of antibacterial properties and low concentrations are sufficient to exercise bactericidal effects [6]. In the last decades, bioactive sol-gel glasses have been investigated for drug delivery and their characteristic of being osteoconductive makes these materials particularly suitable in the prosthetics field [7, 8]. Silicate and calcium silicate glasses and ceramics have been used in many biomedical applications. They stimulate osteogenesis with soluble silica and calcium ions that activate osteoprogenitor cells in the implant site, promoting bone tissue growth [9]. Also these materials have demonstrated the ability to form hydroxyl-apatite on their surface *in*

vitro [10, 11]. This feature is critical to their osseointegration. The sol-gel method can be associated with many coating techniques e.g. dip, spin or spray coating. Many papers describe the use of the sol-gel dip coating technique, which is able to modify the surfaces of some metals with the aim of increasing their bioactivity and biocompatibility [12, 13]. Moreover the coating protects the metal from corrosion and prevents the release of cytotoxic ions [14]. In this work, calcium silicate glasses with increasing percentages of silver oxide have been synthesized by the sol–gel method and used to dip coat titanium grade 4 substrates. Titanium was chosen as the substrate because of its wide variety of applications for implants. Biocompatibility, bioactivity and antimicrobial properties of the obtained coatings have been evaluated by means of in vitro tests and as function of the Ag-content. The purpose has been to identify coatings with high antibacterial activities and osteoconductivities to be used in the prosthetics field. The paper reports also the FTIR analysis of the materials used to make the coating and the study of their thermal behavior performed by simultaneous thermogravimetry/differential thermal analysis (TG/DTA).

2. Materials and Methods

2.1. Sol gel synthesis

Sol-gel glasses were synthesized starting from tetraethyl orthosilicate (TEOS, $Si(OC_2H_5)_4$, Sigma Aldrich), calcium nitrate tetrahydrate ($Ca(NO_3)_2 \cdot 4H_2O$, Sigma Aldrich) and silver nitrate ($AgNO_3$, Sigma Aldrich) as sources of SiO_2, CaO and Ag_2O respectively. Ethanol (EtOH, 99,8% Sigma-Aldrich) and subsequently TEOS were added, under stirring, to a solution of distilled water and nitric acid (HNO_3 ≥65%, Sigma-Aldrich). This solution was prepared using the following molar ratio: TEOS:EtOH:H_2O:HNO_3 = 1:5:1:1. The solution obtained was stirred for 30 min and, then it was added, drop by drop, to a mixture of $Ca(NO_3)_2 \cdot 4H_2O$ and $AgNO_3$ solubilized in ethanol, with a molar ratio $Ca(NO_3)_2$ $4H_2O$:

EtOH = 1:22. The final composition of the gel glasses containing small and increasing amounts of Ag_2O are represented in Table 1 along with the acronyms used.

The sols were stirred for 3h at room temperature and, then, kept at room temperature and away from dust for 24 hours. Titanium grade 4 (Ti-4) disks (Sweden & Martina, Padua, Italy) of 8 mm diameter, equipped with a pin for the attachment of the dip coater clip (KSV LM, Stockholm, Sweden) were used as substrates for dip coating. Ti-4 disks were cleaned in the ultrasonicator with acetone, passivated with HNO_3 ≥65% (Sigma-Aldrich) for 60 min and finally stored in ethanol 99.8%. The substrates were dried in an oven at 50 °C before being dip coated using the obtained sol. After various trials, the extraction speed (V_e) of disks from the sols was set at 10 mm/min and the coated substrates were heat-treated at 50°C for 1 hour to promote film densification. The residual sols, after the dip coating procedure, were left to gel and the obtained materials were heat-treated at 50°C in an oven to obtain the solid samples to be used for chemical characterization and thermal analysis. The flow chart of the process is shown in Fig. 1.

2.2. FTIR Analysis of the synthesized materials

Pulverized samples were analysed using Fourier Transform Infrared Spectroscopy (FTIR) to characterize the chemical interactions between the components. Transmittance FTIR spectra were recorded in the 400-4000 cm^{-1} region using a Prestige 21 spectrophotometer (Shimadzu, Tokyo, Japan) equipped with DTGS KBr (Deuterated Tryglycine Sulphate with potassium bromide windows) detector, with a resolution of 2 cm^{-1} (45 scans). FTIR spectra were analysed by Prestige software (IRsolution).

2.3. Thermal analysis characterization

The thermal behavior of the gels was investigated by using a Stanton Redcroft STA-1500 simultaneous TG/DTA apparatus, consisting of two Pt crucibles of cylindrical shape (with Pt-

Pt/Rh thermocouples): the reference crucible was covered with about 20-25 mg of alumina, while that of the sample (whose size was approximately of 20-25 mg), was first filled with the minimum amount to uniformly cover its bottom surface area to avoid any possible reaction between the sample and Pt at high temperature. TG/DTA experiments were carried out under inert Ar atmosphere (50 ml min^{-1}) at a constant heating rate of 10 K min^{-1} from room temperature to 1200°C. For the kinetic study, TG experiments carried out at heating rates of 5, 7, 10 and 15 °C min^{-1} (under the same gas atmosphere used for thermal behavior study). TG data related to mass losses recorded during the occurrence of dehydration and dehydroxylation were exported in ASCII format before being processed. Calibration of sample temperature was performed using very pure indium and zinc reference materials and a final average uncertainty of ±0.5K was estimated over the whole temperature range.

2.4. SEM of the coatings

Scanning electron microscopy (SEM, Quanta 200, FEI, The Netherlands) was used to investigate the coatings morphologies. The samples were fixed on aluminum stubs using colloidal graphite; the metallization process was not necessary because these samples are good conductors.

2.5. Biological and antibacterial characterization

The evaluation of the bioactivity of the coatings was carried out *in vitro* by soaking the samples for 21 days in a Simulated Body Fluid (SBF) as proposed by Kokubo et al. [15]. SBF is a solution with an ion composition almost equal to those of the human blood plasma buffered at physiological pH 7.40 with HEPES/NaOH. Coated disks were soaked in SBF and kept in a static bath at 37°C. The ratio between the exposed surface of the disks and the SBF volume was fixed equal to 10. The solution was exchanged every 2 days to avoid depletion of the ionic species. After 21 days the samples were removed from SBF, gently rinsed with

ethanol and dried in a desiccator. The surface of the films was analyzed with SEM equipped with Energy Dispersive X-ray (EDX) spectroscopy. The bioactive response of coatings was evaluated in terms of the hydroxyapatite (HA) layer formation on the surface of the samples.

The biocompatibility properties of films were evaluated *in vitro* using NIH 3T3 murine fibroblasts cells (ATCC, VA, USA). Cells were seeded onto coated Ti-4 substrates and their viability was tested with the WST-8 Assay (Dojindo Molecular Technologies Inc., MD, USA). The coated disks were sterilized with 70% ethanol and UV for 12 hours and afterwards placed on the bottom of a polystyrene 24-well plate. Cells were amplified in DMEM medium (Gibco, CA, USA) with 10% (v/v) fetal bovine serum, 1% pen-strep, in a humidified incubator, at 37 °C and 5% CO_2. For each system 3 disks were used and 5000 cells were plated on each disk. Uncoated titanium disks were used as a negative control and the cells grown on the polystyrene wells have been considered to represent 100% viability.

The cells were seeded on disks and after 24 hours they were washed 3 times with PBS (phosphate buffered saline) and again incubated with 10% v/v of WST-8 in a fresh medium for 2 hours. WST-8 is a colorimetric assay and the number of viable cells is directly proportional to the absorbance value (450nm). The absorbance value was measured with a UV-visible spectrophotometer (Biomate 3, Thermo Scientific). For instrument calibration a culture medium with 10% v/v of WST-8, incubated for 24 hours without cell was used.

Staphylococcus aureus (ATCC 25923) was used in this study to test the antibacterial property of the coatings and Tryptone soya broth (TSB, OXOID, England) was used as culture media. Sterilized coated disks were placed in a 24-well plate and incubated with 1ml of bacteria/TSB solutions ($1.0 \cdot 10^5$ bacteria/ml) for 24h at 37 °C. Afterwards the samples were gently rinsed in PBS and fixed in glutaraldehyde 2,5% $_{v/v}$ for 15 min. Bacterial adhesion and proliferation on films was assessed with Environmental Scanning Electron Microscopy (ESEM, Quanta 200, FEI). Uncoated disk was used as a negative control. The operation principle of this microscope is similar to that of classic SEM but it does not require the use of

dehydrated and metallized samples. ESEM allows the observation of a biological sample under "environmental" conditions, maintaining a relative humidity of about 70%. The processes of dehydration and metallization can cause a change of morphology or other artifacts in biological samples [16]. The observation conditions were set at 4 °C and at pressure of 3.6 torr.

3. Results and discussion

3.1. Characterizations of the materials

Fig. 2 shows the FTIR spectra of the synthesized samples (Figure 2B) compared to those of pure SiO_2, pure $Ca(NO_3)_2$ and $AgNO_3$ (Fig. 2a). The bands at 3440 and 1640 cm^{-1}, due to the stretching and bending modes of the hydration water, are found in both the FTIR spectra of the salts and in those of samples. In the spectra of the synthesized materials all the typical peaks of pure SiO_2 are also shown. The bands at 1080, 800 and 460 cm^{-1} are due to the asymmetric and symmetric stretching vibrations and bending mode of Si-O-Si, respectively [17, 18]. However, comparing the spectrum of pure SiO_2 (Fig. 2a) with those of the four 70S30CxA samples (Fig. 2b), a different shape and position of these bands have been observed. In particular, the introduction of Ca^{2+} and Ag^{+} ions into the structure of pure SiO_2 caused the modification of the Si-O-Si network and an increase of the non-bridging oxygen atoms. These transformations lead to a shift of the Si-O signal to lower wavenumbers: the spectra of all the 70S30CxA show a peak at 1050 cm^{-1} (instead of that at 1080 cm^{-1}). The Ag content affects the position of the band ascribed to the stretching of Si-OH bonds. This signal is observed in the range 930-940 cm^{-1} since it shifts to higher wavenumbers with an increase of Ag content. The shift can be explained by the exchange of cations bound to non-bridging oxygen atoms (Ca^{2+} or Ag^{+}). It is known, indeed, that the bond strength of the cation with the non-bridging oxygen decreases with an increase of the size of the cation. The reduction of bond strength causes, in turn, the downshift of the related signal. Therefore, since calcium

ions bound to non-bridging oxygen atoms are quite large, Si-OCa bonds are weaker than Si-OH bonds. The result is that the characteristic signal associated to Si-OH bonds (recorded to 950 cm^{-1} in pure SiO_2 spectrum) is found to be shifted to lower wavenumber (930 cm^{-1}). When the amount of Ag^+ ions increases, it replaces a part of Ca^{2+}. As Ag^+ is smaller than Ca^{2+}, the bond strength and, thus, the wavenumber increases with the Ag^+ content. So, the band is found at 940 cm^{-1} for 70S30C0.27A, which has 1wt% of Ag^+ ions.

Moreover, some FTIR bands demonstrate that the starting substances, $Ca(NO_3)_2$ and $AgNO_3$, may be still present in the gels. In fact, the bands at 1435 cm^{-1} and the sharp peak at 1385 cm^{-1} are assigned to the asymmetric and symmetric stretching vibrations of both nitrate ions of $Ca(NO_3)_2$ and $AgNO_3$ [19, 20] . Furthermore, the sharp peak at 817 cm^{-1} is typical for the bending mode of the nitrate ions of $Ca(NO_3)_2$.

The TG/DTA experiments were carried out with the aim of detecting the best temperature(s) for the heat treatment of the gels. Fig. 3(a,b) shows the TG/DTA curves of the four materials carried out up to 1100°C under a stream of Ar. Similar to what has been observed for similar materials in previously studies [21] all samples undergo a three-step degradation process, characterized by two endothermic effects, those of the first and the third ones being particularly evident, while the second, around 280°C is slightly exothermic, as is more evident in the inner plot of Fig. 3b. Only slight differences are observed in the TG and DTA profiles, thus confirming that the thermal behavior is substantially the same regardless the amount of the Ag ions. The first step up to 160°C, which can be seen as an overlap of two steps with a mass loss of about 27%, is attributed to dehydration (loss of water mainly physically absorbed), even if the simultaneous evolution of residual ethanol upon heating cannot be excluded. The second step, accompanied by a 7% of mass loss, has an exothermic effect, often found in literature. Several authors investigated bioactive glass materials with compositions similar to those of the materials tested in this study [21-24] and all ascribe this exothermic effect to the thermal desorption of chemically adsorbed water. A mass loss of

about 12-13% is found in the third step between 390 and 600°C, which, looking at the shape of the corresponding endothermic DTA peak, should reasonably consist of two overlapping processes. Some authors [25, 26] in the past ascribed this step (occurring in calcium silicate gels similar to those examined in this study) to the decomposition of nitrates, which are used in the preparation of sols examined in this study as well as to other undesired components of the starting material. In the temperature range 900-1000°C an exothermic DTA peak without mass changes is attributed to crystallization of a calcium silicate, which could be presumably pseudowollastonite (α-$CaSiO_3$), taking into account the molar ratio Si/Ca of about 2.3, as indicated in literature [25] .

After the heat treatment, the coated Ti-4 disks have been observed by SEM. The micrographs of the thin films are presented in Fig. 4. All coatings show a sponge-bone like morphology and this remarkable feature makes these films suitable for prosthetic and dentistry use.

3.2. Biological and antibacterial properties of the coatings

Coated disks, after 21 days in SBF, show a surface covered by globular crystals (Fig. 5). This morphology is typical of hydroxyl-apatite. EDX spectra confirms the elemental composition of crystals and shows a molar ratio Ca/P equal to 1.6, in agreement with that of the hydroxyl-apatite formula [$Ca_{10}(PO_4)_6(OH)_2$]. The 70S30C0.08A and 70S30C0.14A films show a higher bioactivity than other systems. The results can be explained by the mechanism of hydroxyapatite nucleation on the surface of sol-gel glasses containing cations. As reported in the literature [27, 28], when exposed to SBF, cation-containing silicate glasses and ceramics release ions with positive charge via exchange with H_3O^+ ions in SBF to form Si–OH groups on their surface; this reaction causes a pH increase of SBF solution and, consequently, Si–OH groups are dissociated into negatively charged units $Si–O^-$. These groups combine with Ca^{2+} ions present in the fluid imposing an increase of positive charge on the surface. In addition, Ca^{2+} ions combine with the negative charge of the phosphate ions to form amorphous

phosphate, which spontaneously transforms into hydroxyl-apatite. As Ag^{+} is an ion with a smaller size then Ca^{2+}, it bonds the non-bridging oxygen more strongly than calcium ion and, thus, is exchanged with more difficulty.

The results of cell viability tests are shown in Fig. 7. The value of cells grown on polystyrene was considered as 100%. Cells seeded on uncoated disks show the lowest viability. The presence of the coatings, thus, improves cell viability. However, the 70S30C0.08A film is the most biocompatible, while a slightly decrease of the viability is observed when the cells are seeded on coatings which contain higher Ag-amounts. This phenomenon can be explained by the release of nitrate ions from the coatings. Higher Ag-amounts correspond to a higher amount of residual nitrate in the materials, which can interfere with the cell viability.

Bacterial adhesion and proliferation on films has been assessed with ESEM and micrographs are shown in Fig. 8. It can be noted that the uncoated disk shows a uniform bacteria film whereas the number of bacteria decreases as the percentage of silver contained in the films increases. This result confirms the notorious antibacterial properties of silver containing materials are retained when this are used in coatings and provide support their potential use in orthopaedics or dental field.

4. Conclusions

The sol-gel technique was successfully used to synthesize silver-containing calcium silicate glasses with antibacterial properties. Thermal analysis (TG/DTA techniques in this study) was found to be a useful tool to examine the thermal behavior of these materials over a wide temperature range and to indicate suitable temperatures for thermal pre-treatment. Experimental data have shown that the antibacterial activity is directly proportional to the silver percentage embedded in the calcium silicate matrix. To apply these coatings successfully in the biomedical field their biocompatibility and bioactivity have also been tested. The results showed that the presence of coatings makes the titanium disks more

biocompatible and more bioactive. However, high percentages of silver (like those contained in samples 70S30C0.19A and 70S30C0.27A) adversely affects the biological properties of the coatings.

In conclusion, the best performance in terms of antimicrobial activity and biological properties was shown by the sample 70S30C0.14A.

References

[1] Phillips JE, Crane TP, Noy M, Elliott TSJ, Grimer RJ. The incidence of deep prosthetic infections in a specialist orthopaedic hospital: a 15-year prospective survey. J Bone Joint Surg Br 2006;88:943-8.

[2] Donlan RM, Costerton JW. Biofilms: Survival mechanisms of clinically relevant microorganisms. Clin Microbiol Rev 2002;15:167-93.

[3] Darouiche RO. Treatment of infections associated with surgical implants. N Engl J Med 2004;350:1422-9.

[4] Lew DP, Waldvogel FA. Osteomyelitis. The Lancet;364:369-79.

[5] Hollinger MA. Toxicological Aspects of Topical Silver Pharmaceuticals. Critical Reviews in Toxicology 1996;26:255-60.

[6] Clement JL, Jarret PS. Antibacterial silver. Met-Based Drugs 1994;1:467-82.

[7] Catauro M, Bollino F, Papale F, Gallicchio M, Pacifico S. Synthesis and chemical characterization of new silica polyethylene glycol hybrid nanocomposite materials for controlled drug delivery. Journal of Drug Delivery Science and Technology 2014;24:320-5.

[8] Catauro M, Bollino F, Papale F, Pacifico S, Galasso S, Ferrara C, et al. Synthesis of zirconia/polyethylene glycol hybrid materials by sol-gel processing and connections between structure and release kinetic of indomethacin. Drug Delivery 2014;21:595-604.

[9] Midha S, Kim TB, van den Bergh W, Lee PD, Jones JR, Mitchell CA. Preconditioned 70S30C bioactive glass foams promote osteogenesis in vivo. Acta Biomater 2013;9:9169-82.

[10] Catauro M, Papale F, Roviello G, Ferone C, Bollino F, Trifuoggi M, et al. Synthesis of SiO_2 and CaO rich calcium silicate systems via sol-gel process: Bioactivity, biocompatibility, and drug delivery tests. Journal of Biomedical Materials Research - Part A 2014;102:3087-92.

[11] Catauro M, Bollino F, Veronesi P, Lamanna G. Influence of PCL on mechanical properties and bioactivity of ZrO_2-based hybrid coatings synthesized by sol-gel dip coating technique. Materials Science and Engineering C 2014;39:344-51.

[12] Catauro M, Bollino F, Papale F, Mozetic P, Rainer A, Trombetta M. Biological response of human mesenchymal stromal cells to titanium grade 4 implants coated with PCL/ZrO_2 hybrid materials synthesized by sol-gel route: In vitro evaluation. Materials Science and Engineering C 2014;45:395-401.

[13] Catauro M, Papale F, Bollino F. Characterization and biological properties of TiO_2/PCL hybrid layers prepared via sol–gel dip coating for surface modification of titanium implants. Journal of Non-Crystalline Solids 2015;415:9-15.

[14] Catauro M, Bollino F, Papale F, Giovanardi R, Veronesi P. Corrosion behavior and mechanical properties of bioactive sol-gel coatings on titanium implants. Materials Science and Engineering C 2014;43:375-82.
[15] Kokubo T, Takadama H. How useful is SBF in predicting in vivo bone bioactivity? Biomaterials 2006;27:2907-15.
[16] Cafiero G, Papale F, Grimaldi A, Rosso F, Barbarisi M, Tortora C, et al. Immunogold labelling in environmental scanning electron microscopy: Applicative features for complementary cytological interpretation. Journal of Microscopy 2010;241:83-93.
[17] Catauro M, Bollino F, Papale F, Gallicchio M, Pacifico S. Influence of the polymer amount on bioactivity and biocompatibility of SiO_2/PEG hybrid materials synthesized by sol-gel technique. Materials Science and Engineering C 2015;48:548-55.
[18] Piccirillo AM, Borysenko SS, Borysenko SD. Qualitative analysis behaviour of the solutions of impulsive differential systems. AAPP Atti della Accademia Peloritana dei Pericolanti, Classe di Scienze Fisiche, Matematiche e Naturali 2011;89.
[19] Irish DE, Walrafen GE. Raman and infrared spectral studies of aqueous calcium nitrate solutions. J Chem Phys 1967;46:378-84.
[20] Piccirillo AM, Ciarletta M, Borysenko SD. Impulsive wendroff's type inequalities and their applications. AAPP Atti della Accademia Peloritana dei Pericolanti, Classe di Scienze Fisiche, Matematiche e Naturali 2012;90.
[21] Oki A, Parveen B, Hossain S, Adeniji S, Donahue H. Preparation and in vitro bioactivity of zinc containing sol-gel–derived bioglass materials. Journal of Biomedical Materials Research Part A 2004;69A:216-21.
[22] Riti PI, Vulpoi A, Ponta O, Simon V. The effect of synthesis route and magnesium addition on structure and bioactivity of sol–gel derived calcium-silicate glasses. Ceramics International 2014;40:14741-8.
[23] Siqueira RL, Peitl O, Zanotto ED. Gel-derived SiO_2–CaO–Na_2O–P_2O_5 bioactive powders: Synthesis and in vitro bioactivity. Materials Science and Engineering: C 2011;31:983-91.
[24] Bellucci D, Sola A, Salvatori R, Anesi A, Chiarini L, Cannillo V. Sol–gel derived bioactive glasses with low tendency to crystallize: Synthesis, post-sintering bioactivity and possible application for the production of porous scaffolds. Materials Science and Engineering: C 2014;43:573-86.
[25] Saravanapavan P, Hench LL. Mesoporous calcium silicate glasses. I. Synthesis. Journal of Non-Crystalline Solids 2003;318:1-13.

[26] Meiszterics A, Sinkó K. Sol–gel derived calcium silicate ceramics. Colloids and Surfaces A: Physicochemical and Engineering Aspects 2008;319:143-8.
[27] Takadama H, Kim H-M, Kokubo T, Nakamura T. X-ray photoelectron spectroscopy study on the process of apatite formation on a sodium silicate glass in simulated body fluid. J Am Ceram Soc 2002;85:1933-6.
[28] Ohtsuki C, Kokubo T, Yamamuro T. Mechanism of apatite formation on $CaOSiO_2P_2O_5$ glasses in a simulated body fluid. Journal of Non-Crystalline Solids 1992;143:84-92.

Table 1 Labels and composition of the synthesized gels

Acronym	SiO_2/$\%_{mol/mol}$	CaO/$\%_{mol/mol}$	Ag_2O/	
			$\%_{mol/mol}$	$\%_{w/w}$
70S30C0.08A	69.94	29.98	0.08	0.30
70S30C0.14A	69.90	29.96	0.14	0.50
70S30C0.19A	69.87	29.94	0.19	0.70
70S30C0.27A	69.81	29.92	0.27	0.99

Captions to figures:

Fig. 1 Flow chart of sol-gel procedure

Fig. 2 FTIR spectra of **a)** pure SiO_2 and pure salts used in the synthesis process; **b)** 70S30CxA synthesized gels, where: 0.08A = 70S30C0.08A; 0.14A = 70S30C0.14A; 0.19A = 70S30C0.19A; 0.27 = 70S30C0.27A.

Fig. 3 TG/DTA curves of the four 70S30CxA synthesized gels at 10K/min under a stream of argon.

Fig. 4 SEM micrographs of coatings

Fig. 5 Coated surface after 21 days in SBF. EDX spectra confirms the elements composition of globular crystals

Fig. 6 WST-8 assay value: cells grown on polystyrene were considered 100% viable, uncoated titanium shows the lowest viability value.

Fig. 7 *S. Aureus* on coated titanium

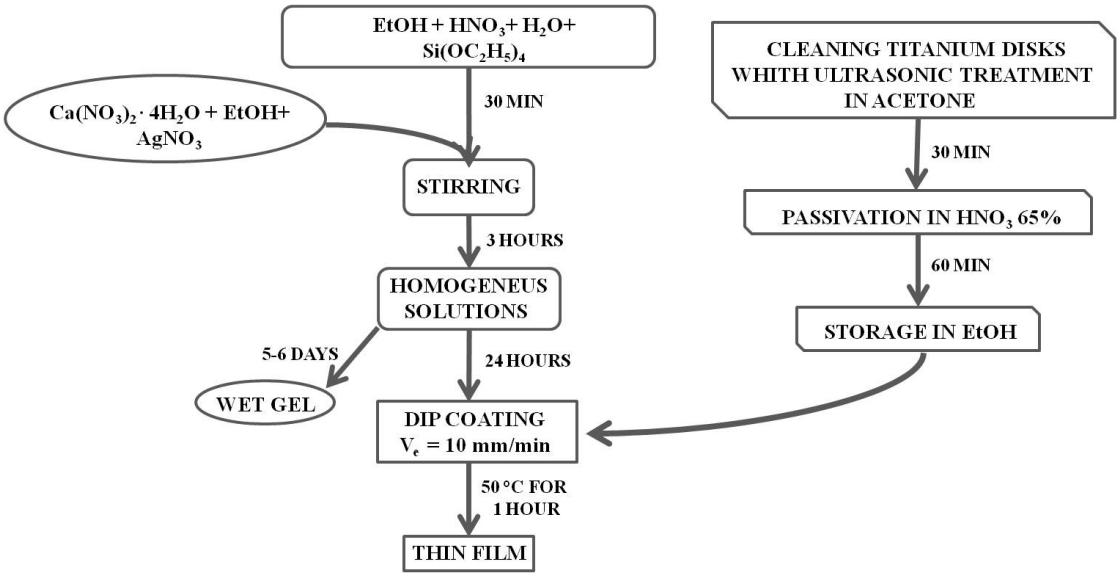
EtOH + HNO3+ H2O+ Si(OC2H5)4
Ca(NO3)2 · 4H2O + EtOH+ AgNO3
30 MIN
STIRRING
3 HOURS
HOMOGENEUS SOLUTIONS
5-6 DAYS
WET GEL
24 HOURS
DIP COATING Ve = 10 mm/min
50 °C FOR 1 HOUR
THIN FILM
CLEANING TITANIUM DISKS WHITH ULTRASONIC TREATMENT IN ACETONE
30 MIN
PASSIVATION IN HNO3 65%
60 MIN
STORAGE IN EtOH

Fig 1

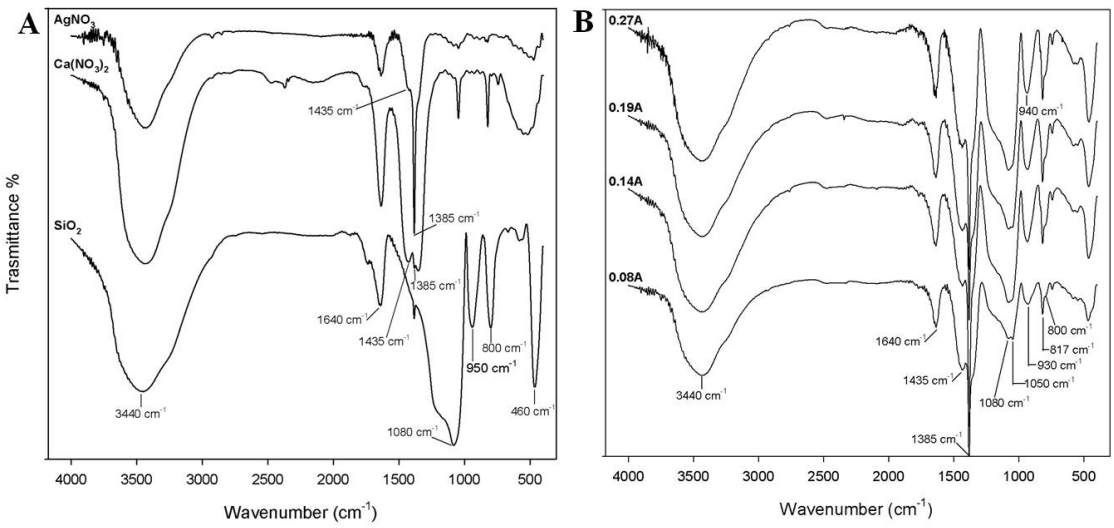
A
AgNO3
Ca(NO3)2
SiO2
1435 cm-1
1385 cm-1
1640 cm-1
800 cm-1
950 cm-1
3440 cm-1
1080 cm-1
460 cm-1
Trasmittance %
Wavenumber (cm-1)
B
0.27A
0.19A
0.14A
0.08A
940 cm-1
1640 cm-1
1435 cm-1
1385 cm-1
1080 cm-1
3440 cm-1
800 cm-1
817 cm-1
930 cm-1
1050 cm-1
Wavenumber (cm-1)

Fig 2

Fig 3

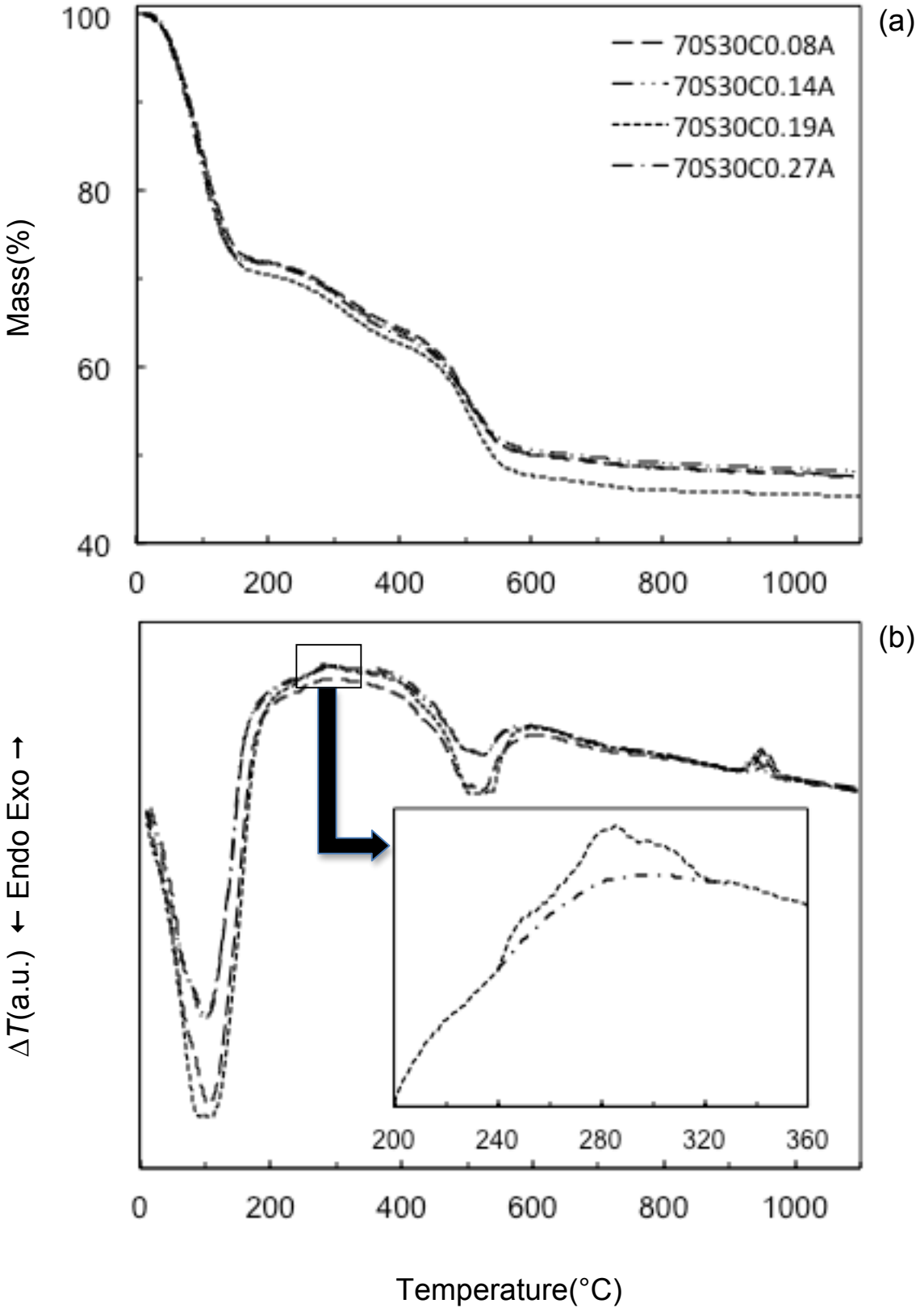
(a)
100
80
60
40
Mass(%)
70S30C0.08A
70S30C0.14A
70S30C0.19A
70S30C0.27A
0
200
400
600
800
1000
(b)
ΔT(a.u.) ← Endo Exo →
200
240
280
320
360
Temperature(°C)

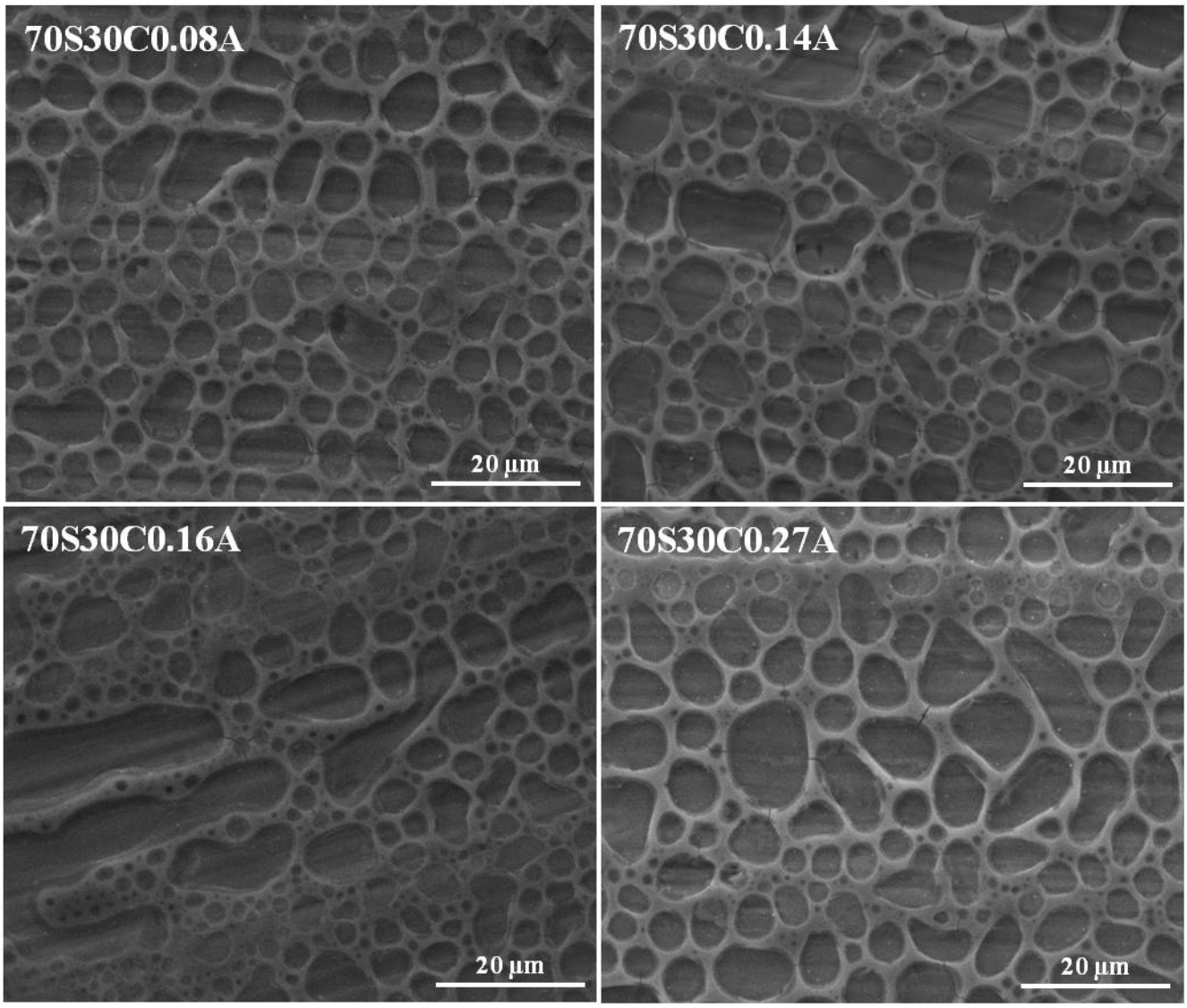
70S30C0.08A
20 µm
70S30C0.14A
20 µm
70S30C0.16A
20 µm
70S30C0.27A
20 µm

fig 4

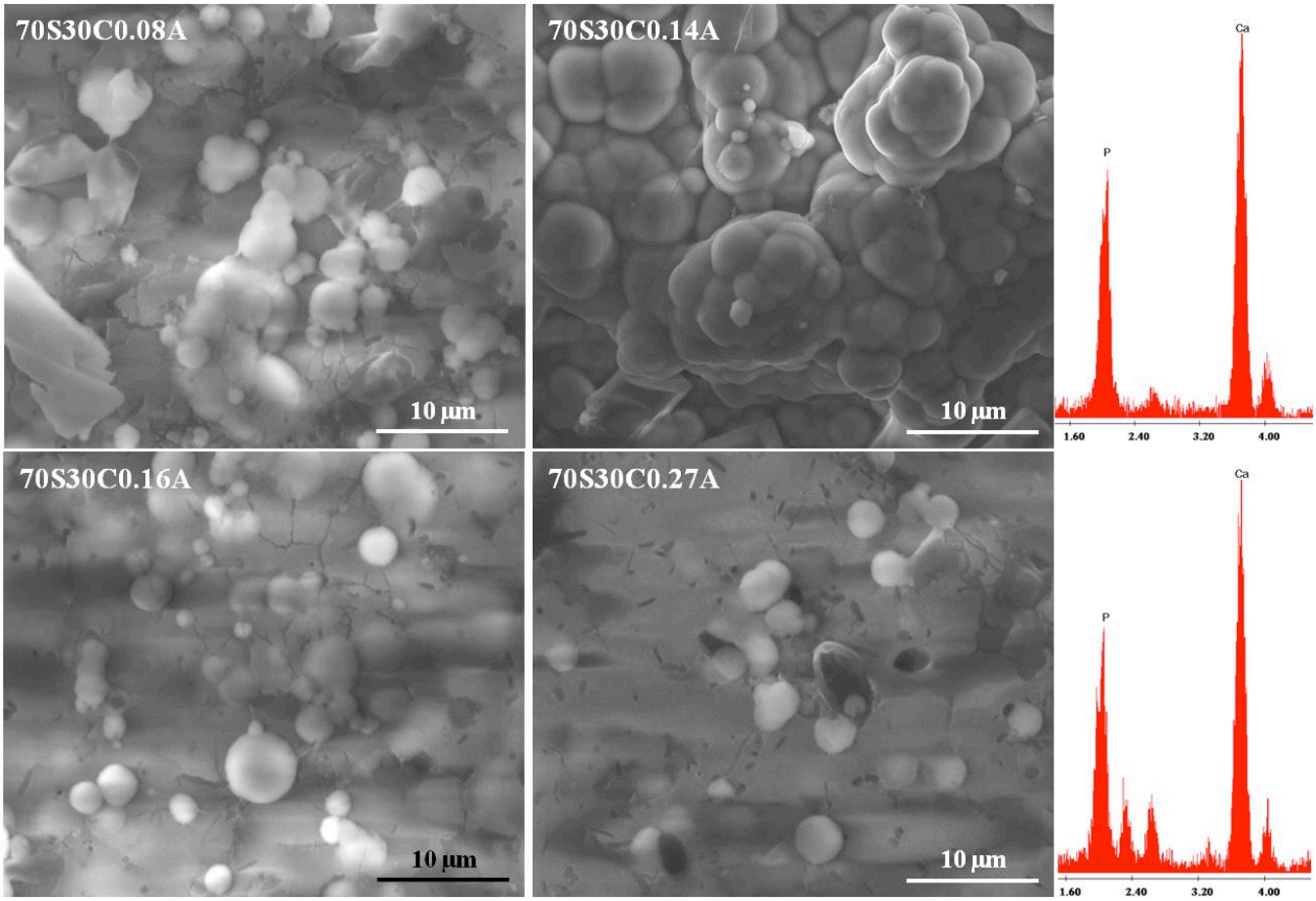
70S30C0.08A
10 µm
70S30C0.14A
10 µm
Ca
P
1.60
2.40
3.20
4.00
70S30C0.16A
10 µm
70S30C0.27A
10 µm
Ca
P
1.60
2.40
3.20
4.00

fig 5

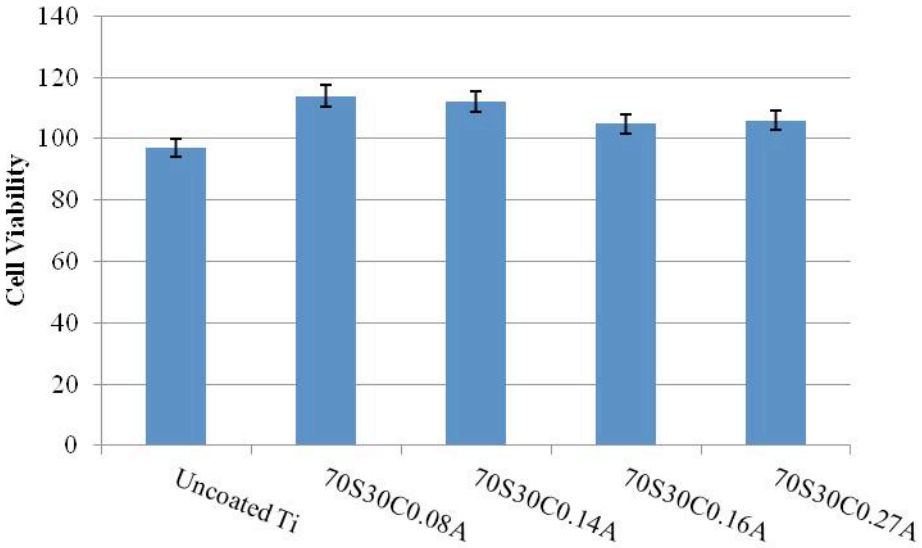
140
120
100
80
60
40
20
0
Cell Viability
Uncoated Ti
70S30C0.08A
70S30C0.14A
70S30C0.16A
70S30C0.27A

Fig 6

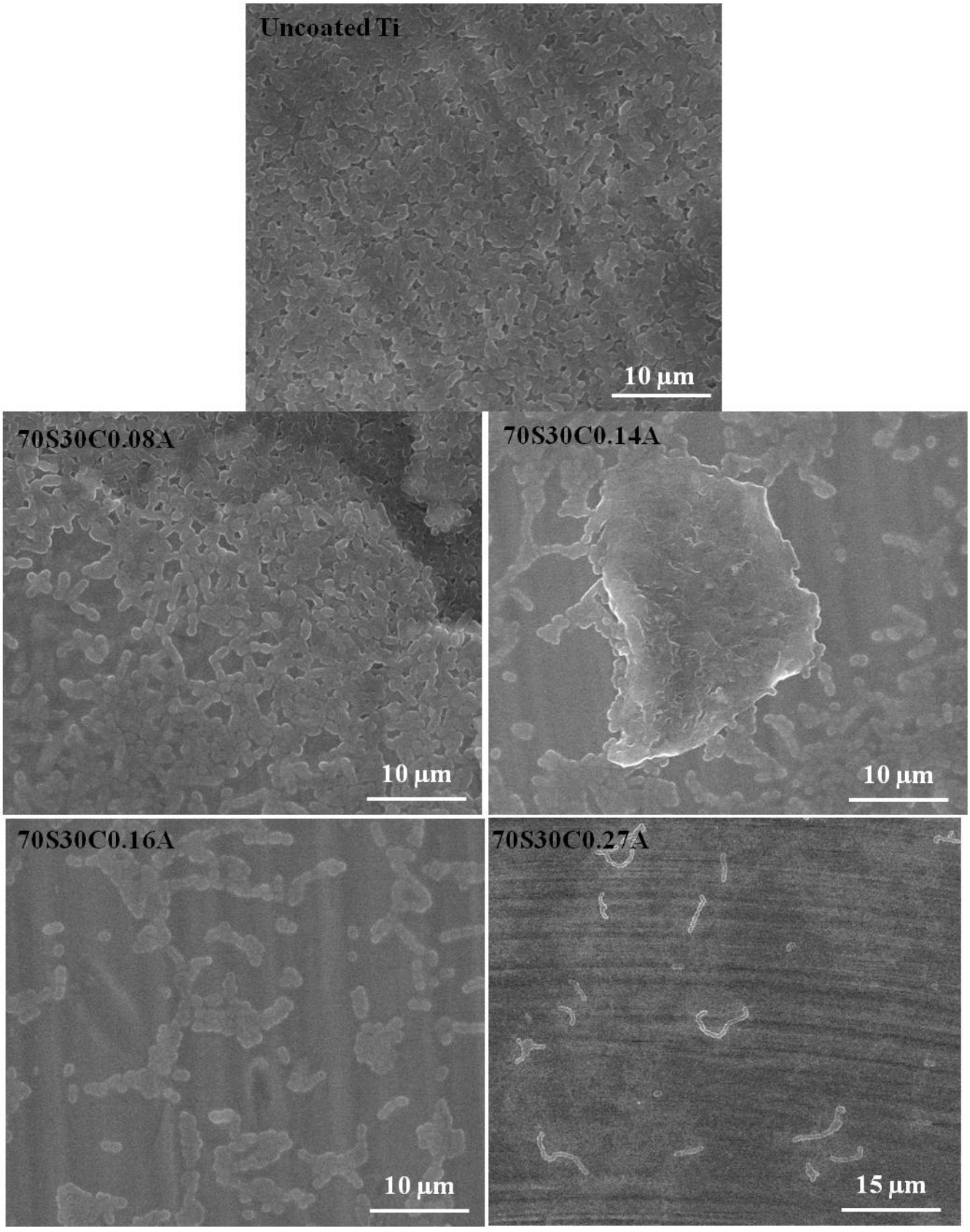
Uncoated Ti
10 µm
70S30C0.08A
10 µm
70S30C0.14A
10 µm
70S30C0.16A
10 µm
70S30C0.27A
15 µm

fig 7